Modeling of Interface Crack Growth using Discontinuous Galerkin Method

Felicia Stan[1, a]

[1]Dunarea de Jos University of Galati, 47 Domneasca, 800008, Galati, Romania

[a]felicia.stan@ugal.ro

Keywords: discontinuous Galerkin finite element method, interface fracture, cohesive law.

Abstract. This paper presents the discontinuous Galerkin (dG) method with interior penalties and its implementation for the interface crack growth. The interface fracture is modeled using cohesive zone models. The discontinuous Galerkin method is a finite element method, which uses discontinuous, piecewise polynomial spaces for the numerical solution and the test functions. The method is endowed with several features including flexibility and stability with respect to adaptivity of mesh and polynomial approximations. A numerical example is presented to illustrate the ability of the dG method to accurately model interface cracking phenomena. Numerical evidence suggests the absence of spurious traction oscillations when discontinuous Galerkin method is used in conjunction with cohesive models. Compared to conventional interface elements, the discontinuous Galerkin method has the advantage of allowing crack formation without insertion of cohesive elements during the simulation.

Introduction

The interface fracture phenomena play an important role in a number of applications especially in laminate composite systems. Frequently, singular forces are supported on these interfaces (e.g. surface tension forces) and material parameters might be discontinuous across the interface. Delamination (interlamiar damage) is a typical kind of interface fracture phenomena which occurs in laminate materials (see Fig. 1), often accompanied with transverse matrix cracking or fiber fracture (intralaminar damage).

When modeling interface fracture phenomena, the standard way to solve fracture problems with finite element methods consists of inserting interface elements (see Fig. 1) with zero thickness in the mesh at places where cracking is expected to occur [1, 2, 3]. A main advantage of the use of interface elements is the capability to predict both onset and propagation of delamination without previous knowledge of the crack location and propagation direction.

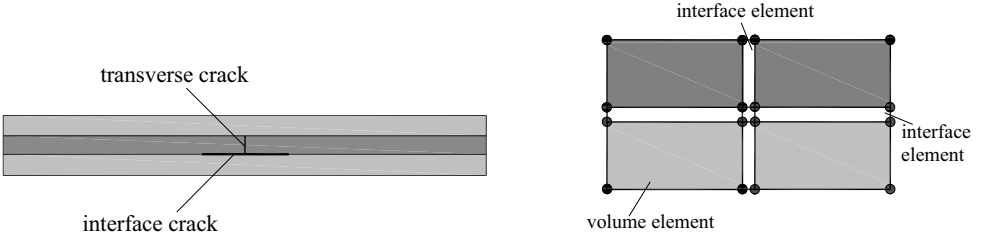

Fig. 1. Modeling of interface fracture

From a modeling perspective, a major drawback of the use of interface elements is that the insertion of cohesive elements introduces an artificial compliance in the structure which is primarily related to the initial slope of the traction-separation law: a stiffer slope introduces a higher initial rigidity between neighboring bulk elements, thus resulting in a smaller fictitious compliance.

On the other hand, a high elastic stiffness of the cohesive surface compared to the elastic stiffness of the bulk material can result in artificial oscillations prior to the opening of the cohesive surface. Moreover, some interface elements require a special topology when they are applied in conjunction with solid-like shell elements [3].

The need to develop a computational procedure for interface fracture phenomena that retains the advantages of the cohesive models is therefore self-evident. A candidate approach is the class of discontinuous Galerkin methods, which have recently shown promise in a variety of solid mechanics problems.

The discontinuous Galerkin method is a class of finite element methods, which uses discontinuous, piecewise polynomial spaces for the numerical solution and the test functions. The discontinuous Galerkin method was first proposed in 1973 for approximating the neutron transport problems by Reed and Hill [4]. Since then important contribution were given by Douglas and Dupont [5], Wheeler [6], and Arnold [7] who extended the Nitsche [8] approach to weakly enforce the continuity of the solution at interior edges: jump terms in the unknown variable across internal boundaries were introduced, and the jump terms were penalized to enforce continuity across the element interface. A comprehensive description of discontinuous Galerkin methods can be found in [9]. Within the context of elasticity, in recent years, there have been important contributions by Zienkiewicz et al. [10], Riviere, et al. [11], Epshteyn and Rivière [12] Lew et al. [13], Eyck and Lew [14].

The main features of discontinuous Galerkin methods are: (i) the weighting and trial functions are identical (ii) the discontinuous Galerkin methods are locally mass conservative at the element level - the element topology, the degree of approximation and even the choice of governing equations can vary from element to element and in time over the course of calculation without loss of rigor in the method; (iii) the discontinuous Galerkin methods capture the discontinuity in the solution very well by the nature of discontinuous function space; thus, the these methods are naturally suited for the application within the computational interface. A particularly powerful combination is to couple dG method with cohesive law; (iv) from a computer point of view, the simple communication pattern between elements makes discontinuous Galerkin method potentially being well parallelizable.

The obvious disadvantage of the DG method is the increased number of degrees of freedom for the same order of approximation. Thus, another disadvantage of DG methods is its high storage and high computational requirements.

The main objective of this paper is to develop and implement a numerical scheme aimed at modeling interface fracture phenomena using discontinuous Galerkin method. The resulting discontinuous Galerkin weak form naturally leads to the implementation of cohesive models. The performances of the discontinuous Galerkin method for interfacial fracture problems are demonstrated through a numerical example.

Problem statement and weak formulation

Consider the boundary value problem of a general three-dimensional body $\Omega \subset \Re^3$ in equilibrium such that in Fig. 2. The body is supported on the area $\partial_D\Omega$ with prescribed displacements and is subjected to surface tractions on the surface area $\partial_N\Omega$. In addition, the body is subjected to externally applied body forces b. The continuum problem is governed by the following equations stated in terms of the Cauchy stress

$$\begin{aligned} -\nabla\cdot\sigma &= b \quad \text{in } \Omega \\ u &= g_D \quad \text{on } \partial_D\Omega \\ \sigma\cdot n &= g_N \quad \text{on } \partial_N\Omega \end{aligned} \tag{1}$$

in which σ is the stress tensor, ∇ is the gradient operator, u is displacement vector, n is the unit normal vector to the surface, and g_D and g_N are the boundary conditions applied on the displacement $\partial_D\Omega$ and traction $\partial_N\Omega$ parts of the boundary, respectively.

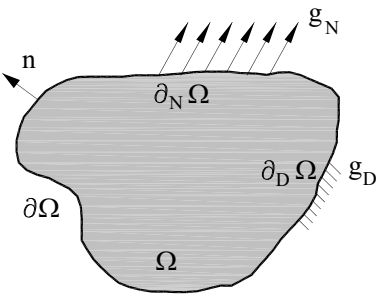

Fig. 2. Body with prescribed displacements and traction conditions

Let $\Omega_h = \{K\}$ be a shape-regular partition of Ω, where K are finite elements. The reference configuration Ω is approximated by Ω_h such that

$$\Omega \sim \Omega_h = \bigcup_{e=1}^{E} \Omega^e, \ \overline{\Omega}^e \bigcap_{\forall e \neq e'} \overline{\Omega}^{e'} = 0 \tag{2}$$

where $\overline{\Omega}^e$ represents the interior of sub-domain Ω^e. It is assumed that Ω_h satisfies the necessary admissibility and Lipschitz continuity conditions [10].

A finite-dimensional piecewise polynomial approximation of the field u is defined on Ω_h by introducing the following space [10]:

$$V_h^k = \left\{ u_h \in L^2(\Omega_h) : u_h|_{\Omega^e} \in P^k(\Omega^e) \ \ \forall \in \Omega_h \right\} \tag{3}$$

where $P^k(\Omega^e)$ is the space of polynomial functions of order up to k with support in Ω^e. The polynomial order approximation is the same for all unknown fields. These spaces differ from the conventional finite element spaces in that they allow for jump discontinuities at inter-element boundaries of polynomial order k. To construct a numerical scheme with high order accuracy in the vicinity of discontinuities, we require all discontinuities to lie on element boundaries, Fig. 3.

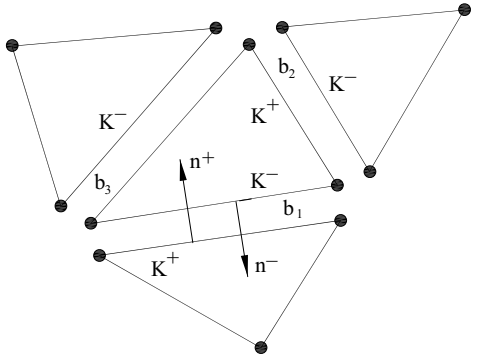

Fig. 3. Discontinuous finite element mesh

Let b denote an arbitrary element edge, and $\Gamma = \{b\}$, $b = b^+ \cap b^-$, be the set of all edges. Each element boundary b is shared by two elements K^+ and K^- such that $b = K^+ \cap K^-$, with n^+ being the unit outward normal vector to element K^+ (see Fig. 3).

The set of all edges Γ is decomposed into three disjoints subsets such that $\Gamma = \Gamma_I \cup \Gamma_D \cup \Gamma_N$, where Γ_I is the set of all internal edges, $\Gamma_I = \{b \in \partial K \setminus \partial\Omega : K \in \Omega_h\}$; Γ_D is the set of all element edges on the Dirichlet part of the boundary $\partial_D\Omega$, $\Gamma_D = \{b \subset \partial K \cap \partial_D\Omega : K \in \Omega_h\}$; Γ_N is the set of all element edges on the Neumann part of the boundary $\partial_N\Omega$, $\Gamma_N = \{b \subset \partial K \cap \partial_N\Omega : K \in \Omega_h\}$.

The definitions of the average and jump are given by

$$\langle x \rangle = \begin{cases} \frac{1}{2}\left(x^+ + x^-\right) & \forall x \in \Gamma_I \\ x^+ & \forall x \in \Gamma_D \cup \Gamma_N \end{cases} \tag{4}$$

$$[x] = \begin{cases} x^+ - x^- & \forall x \in \Gamma_I \\ x^+ & \forall x \in \Gamma_D \cup \Gamma_N \end{cases} \tag{5}$$

We have assumed that $n^+ = -n^- \ \forall x \in \Gamma_I$. The + and – superscripts correspond to evaluating the function at either side of the edge b.

If the Dirichlet boundary conditions are enforced weakly, the resulting stabilized problem can be written as finding $u_h \in V_h^k$ such that $\forall v \in V_h^k$ [11, 12]:

$$B(v, u_h) = L(v; b) \tag{6}$$

in which

$$\begin{aligned} B(v, u_h) = {} & \left(\varepsilon(v), \sigma(u_h)\right)_K - \left([v], \langle \sigma(u_h) \cdot n \rangle\right)_{\Gamma_I} + \alpha\left(\langle \sigma(v) \cdot n \rangle, [u_h]\right)_{\Gamma_I} - \left(v, \sigma(u_h) \cdot n\right)_{\Gamma_D} + \\ & + \alpha\left(\sigma(v) \cdot n, u_h\right)_{\Gamma_D} + \left(\tau[v], [u_h]\right)_{\Gamma_I} + \left(\tau v, u_h\right)_{\Gamma_I} \end{aligned} \tag{7}$$

$$L(v; b) = (v, b)_K - \left(v, g_N\right)_{\Gamma_N} + \alpha\left(\sigma(v) \cdot n, g_D\right)_{\Gamma_D} + \left(\tau v, g_D\right)_{\Gamma_D} \tag{8}$$

In the above equations τ is the penalty parameter defined by

$$\tau = \frac{\beta}{h_e} \tag{9}$$

where β is positive constant (assumed sufficiently large), and h_e is the characteristic length of the mesh obtained from the two neighboring elements as [11]

$$h_e = \min\left(\frac{L_{K^-}}{A_{K^-}}, \frac{L_{K^+}}{A_{K^+}}\right) \tag{10}$$

in which L is the length of an element edge and A is the area of an element K.

The parameter α is either +1, or -1, corresponding to non-symmetric [7, 9] and symmetric interior penalty methods [6, 9], respectively. The last two terms in Eq. (7) are commonly considered to enhance the stability of the method.

Finite element implementation

The interpolation of the displacement and its jump is accomplished with standard finite element shape functions $N(\xi)$, where $\xi = (\xi_1, \xi_2, \xi_3)$ are the natural coordinates,

$$\mathbf{u}_h = \mathbf{N}(\xi)\mathbf{u}_e \tag{11}$$

$$[\mathbf{u}_h] = \mathbf{N}_{b+}(\xi)\mathbf{u}_{b+} - \mathbf{N}_{b-}(\xi)\mathbf{u}_{b-} \tag{12}$$

where $\mathbf{u}_e$ are the nodal degrees of freedom of the element K, $\mathbf{N}_{b+}$ - the standard finite element shape functions for positive internal boundary b^+, $\mathbf{u}_{b+}$ - the nodal degrees of freedom of the positive internal boundary b^+.

The average of projected gradients of test and trial functions is interpolated using the same technique

$$\left\langle \nabla^s \mathbf{u}_h \cdot \mathbf{n} \right\rangle = \frac{1}{2}\left[\nabla^s \mathbf{N}_{b+}(\xi)\,\mathbf{n}_{b+}(\xi)\mathbf{u}_{b+} + \nabla^s \mathbf{N}_{b-}(\xi)\,\mathbf{n}_{b-}(\xi)\mathbf{u}_{b-}\right] \tag{13}$$

in which $\mathbf{n}_{b+}$ is the inter-element outer surface normal corresponding to element K^+ (see Fig. 3).

When interpolations (11)-(12) are inserted in Eq. (7), the following expression for the bilinear form is obtained:

$$\begin{aligned} &\int_K \mathbf{B}_e^T \mathbf{D} \mathbf{B}_e \, d\Omega - \frac{1}{2}\int_{\Gamma_I} \left(\mathbf{N}_{b+}^T - \mathbf{N}_{b-}^T\right)\mathbf{n}\,\mathbf{D}\left(\mathbf{B}_{b+} - \mathbf{B}_{b-}\right) d\Gamma + \alpha\frac{1}{2}\int_{\Gamma_I} \left(\mathbf{B}_{b+}^T - \mathbf{B}_{b-}^T\right)\mathbf{D}\,\mathbf{n}\left(\mathbf{N}_{b+} - \mathbf{N}_{b-}\right) d\Gamma - \\ &- \int_{\Gamma_D} \mathbf{N}_e^T \mathbf{n}\,\mathbf{D}\,\mathbf{B}_e \, d\Gamma + \int_{\Gamma_D} B_e^T \mathbf{D}\,\mathbf{n}^{\,T} N_e \, d\Gamma + \int_{\Gamma_I} \tau_b \left(\mathbf{N}_{b+}^T - \mathbf{N}_{b-}^T\right)\left(\mathbf{N}_{b+} - \mathbf{N}_{b-}\right) d\Gamma + \int_{\Gamma_D} \tau_e \mathbf{N}_e^T \mathbf{N}_e \, d\Gamma \end{aligned} \tag{14}$$

On substituting the interpolation (11) in Eq. (8), the following expression for the linear follows:

$$\int_{\Gamma_D} \mathbf{N}_e^T \mathbf{b} \, d\Gamma + \int_{\Gamma_N} \mathbf{N}_e^T g_N \, d\Gamma + \int_{\Gamma_D} B_e^T \mathbf{D}\,\mathbf{n}^{\,T} g_D \, d\Gamma + + \int_{\Gamma_D} \tau_e \mathbf{N}_e^T g_D \, d\Gamma \tag{15}$$

In the above equations, **D** is the material moduli tensor, and **B** is the matrix of the shape function derivative.

Cohesive interface model

In a cohesive zone model the material separation behavior is described within a softening constitutive equation relating the crack surface tractions to the material separation across the crack. The softening traction–separation law represents the physical processes of material deterioration occurring in the element interface [15].

In the computation an irreversible bilinear cohesive law (see Fig. 4) with loading and unloading was employed [16, 17]. The cohesive law is defined in terms of a non-dimensional effective displacement and effective traction

$$\lambda = \sqrt{\left(\delta_n / \delta_n^c\right)^2 + \left(\delta_s / \delta_s^c\right)^2} \quad \text{and} \tag{16}$$

$$t = \sqrt{t_n^2 + t_s^2}\,, \tag{17}$$

respectively; in which δ_n and δ_s are normal and tangential displacement jumps at the interface estimated by the finite element analysis; δ_n^c and δ_s^c are critical values at which interface failure takes place; t_n and t_s are the normal and tangential tractions, respectively.

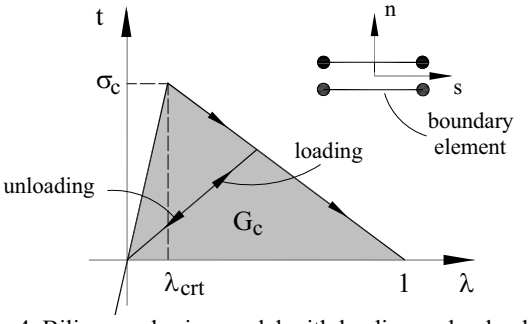

Fig. 4. Bilinear cohesive model with loading and unloading

It is assumed that the traction across the interface increases linearly to its maximum value σ_c which corresponds to a displacement λ_{crt}. In this stage, the stress is linked to relative displacement via interface stiffness. Beyond λ_{crt}, the traction reduce to zero for $\lambda = 1$.

For $0 < \lambda \le \lambda_{crt}$, the shear and normal tractions are defined by

$$t_s = \sigma_c \frac{1}{\lambda_{crt}} \left(\frac{\delta_s}{\delta_s^c}\right) \text{ and } t_n = \sigma_c \frac{1}{\lambda_{crt}} \left(\frac{\delta_n}{\delta_n^c}\right) \tag{18}$$

For $\lambda_{crt} < \lambda < 1$, the tractions across the interface are defined by

$$t_s = \frac{1-\lambda}{1-\lambda_{crt}} \frac{\sigma_c}{\lambda} \left(\frac{\delta_s}{\delta_s^c}\right) \text{ and } t_n = \frac{1-\lambda}{1-\lambda_{crt}} \frac{\sigma_c}{\lambda} \left(\frac{\delta_n}{\delta_n^c}\right) \tag{19}$$

The unloading behavior in the hardening region follows the same slope as the loading path (see Fig. 4). Reloading follows hardening slope and then continues along the softening slope. In the softening region, unloading is assumed to follow a different linear path back from the current position to the origin.

Numerical example

To study the capability of the discontinuous Galerkin method to predict the softening response of a structure given its fracture properties, a single-edge notched beam (SNB) was considered with unstructured mesh. The geometry, the boundary conditions and the mesh used in the study are shown in Fig. 5.

The mesh consists of 127 three-noded triangle elements, 380 nodes, and 380 boundaries, respectively. For the analysis, the following materials properties are used: Young's modulus $E = 3.5 \cdot 10^4$ MPa, Poisson's ration ν=0.15, tensile strength σ_c=3 MPa, fracture energy $G_c = 0.1$ Nmm^{-1}.

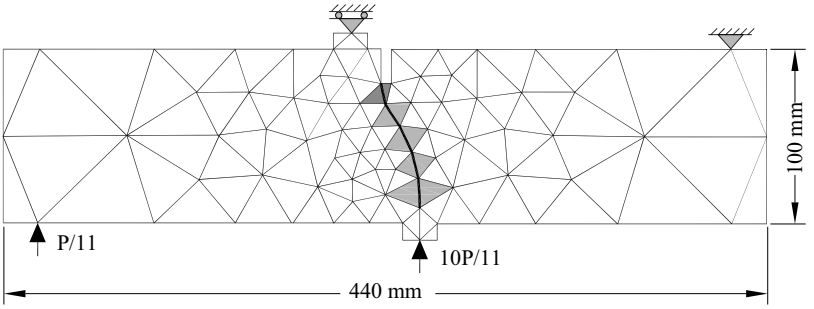

Fig. 5. Geometry, boundaries conditions, and mesh of SEN beam

The discontinuous Galerkin formulation presented above has been implemented using object-oriented programming in C++. The cohesive model can be easily implemented in the discontinuous finite element framework. Within the present formulation, once a crack nucleates along an edge, i.e. the effective traction t, Eq. (17), at each integration point in the elastic region reaches its maximum value σ_c, a cohesive interface is activated, and the relationship between the crack opening displacements and the tractions is governed by Eqs. (18) and (19), respectively. If parameter λ is equal to 1, a crack is introduced along the inter-element boundaries.

The analysis was done considering Gauss integration scheme. For the boundary located at the interface 3-point Gauss integration scheme was used (see gray triangles in Fig. 5) while for the rest of elements 2-point Gauss integration scheme was employed.

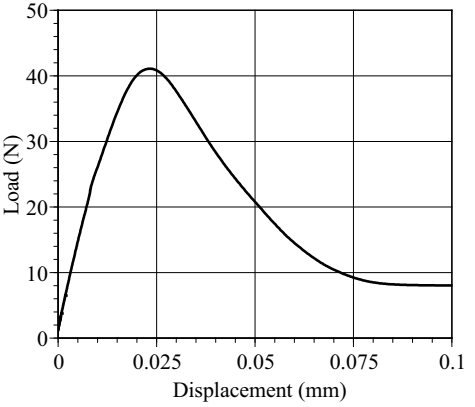

Fig. 6. Load-displacement response for the SEN beam

The predicted crack path is shown in Fig. 5 (the thicker line), while the load-displacement response for the simulation is presented in Fig. 6. The simulation was stop before the complete fracture of the specimen. Although a relative coarse mesh was used, a good convergence was met for every load increment.

Summary

In this paper, a new computational approach based on discontinuous Galerkin method and cohesive zone models to study interface fracture phenomena has been presented and illustrated for a single-edge notched beam. The discontinuous Galerkin method can handle cohesive cracks very naturally with some advantages over the other methods, including good stability and consistency, absence of traction oscillations and spurious reflections. Compared to conventional cohesive elements, the discontinuous Galerkin method has the advantage of allowing crack formation without insertion of cohesive elements during the simulation.

One of the downsides of the discontinuous Galerkin methods is the computational cost since a loop over the boundaries in the mesh in necessary. Also, an important yet unresolved problem is the automatic selection of the stabilization parameter. However, the proposed discontinuous Galerkin finite element formulation with cohesive models can simplify the computational modeling of failure along interfaces.

Acknowledge

The financial support of the NURC-CNCSIS, through the grant AT 113-2008, is gratefully acknowledged.

References

[1] A. Needleman: Int. J. of Fract. Vol. 42 (1990), p.21.

[2] J.J.C. Remmers, R. de Borst, and A. Needleman: Comput. Mech. Vol. 31 (2003), p. 69.

[3] V.K. Goyal, E.R. Johnson, and C.G. Davila: Compos. Struct. Vol. 65 (2004), p. 289.

[4] W. Reed and T. Hill: Tech. report LA-UR-73-479, Los Alamos National Laboratory, Los Alamos, New Mexico, USA (1973).

[5] J. Douglas, Jr. and T. Dupont, in: Lecture Notes in Physics, volume 58, Springer, Berlin (1976).

[6] D.N. Arnold: SIAM J. Numer. Anal. Vol. 19 (1982), p. 742.

[7] M.F. Wheeler, SIAM J. Numer. Anal. Vol. 15 (1978), p. 152.

[8] J. Nitsche: Abh. Math. Sem. Univ. Hamburg, Vol. 36 (1971), p. 9.

[9] B. Cockburn, G.E. Karniadakis, and C.-W. Shu (Eds.), in: Lecture Notes in Computational Science and Engineering, volume 11, Springer, Berlin (2000).

[10] O.C. Zienkiewicz, et all: Int. J. Numer. Meth. Engng. Vol. 58 (2003), p. 1119.

[11] B. Rivière, S. Shaw, M.F. Wheeler and J.R. Whiteman: Numer. Math. Vol. 95 (2003), p. 347.

[12] Y. Epshteyn, and B. Rivière: J. Comput. Appl. Math. (2006), in press.

[13] A. Lew, P. Neff, D. Sulsky, and M. Ortiz: Appl. Math. Research eXpress, Vol. 3 (2004), p. 73.

[14] A.T. Eyck, and A. Lew: Int. J. Numer. Meth. Engng. Vol. 67 (2006), p.1204.

[15] M. Ortiz, and A. Pandolfi: Int. J. Numer. Meth. Engng. Vol. 44 (1999), p. 1267.

[16] H.D. Espinosa, and P.D. Zavattieri: Mech. Mat. Vol. 35 (2003), p. 333.

[17] S.H. Song, H. Paulino, and W.G. Buttlar: Eng. Frac. Mech. Vol. 73 (2006), p. 2829